engineering proceedings

Proceeding Paper

Application of Fourier Analysis for Power Characteristics Determination in Series-Resonant LC Converter †

Dimitar Spirov, Vasil Mihov *, Yasen Madankov and Hristo Vargov

EEEA Department, University of Food Technologies, 4002 Plovdiv, Bulgaria; d_spirov@uft-plovdiv.bg (D.S.); y_madankov@uft-plovdiv.bg (Y.M.); h.vargov@gmail.com (H.V.)

* Correspondence: v_mihov@uft-plovdiv.bg

† Presented at the International Conference on Electronics, Engineering Physics and Earth Science (EEPES2026), Bandirma, Turkey, 24–27 June 2026.

Abstract

This paper presents the behavior of a series-resonant converter. A Fourier harmonic analysis of a second-order circuit topology is presented. Some calculations about the main values of the converter are given. Determination of the power characteristics and efficiency is made by including higher-order harmonics in the analysis. Thus, a more exact simulation of the circuit behavior has been achieved, especially at variable load. The applied method reveals significant deviations compared to the results from the classical first harmonic approximation (FHA). Conduction between theoretical results and experimental data is presented, using a laboratory prototype of a resonant converter circuit. Experimental data confirms the accuracy of the applied higher-order harmonic analysis and highlights its importance for improving the efficiency and reliability of the converters. A conclusion about the benefits of the presented approach, together with some directions about future work, is given.

Keywords: harmonic approximation; power converter; series-resonant converter

1. Introduction

In the study and optimization of converters containing resonant circuits, the evaluation of power distribution and transfer between individual components is a critically important process [1]. Classical analysis approaches often employ the first harmonic approximation (FHA), which, although sufficiently accurate in many cases, does not account for the influence of higher-order harmonics [2,3].

In series-resonant converters, which are widely used in high-power applications, the full spectrum of currents and voltages typically includes a significant number of harmonics. Therefore, in such cases, analysis using only the first harmonic can lead to substantial deviations and, consequently, inaccurate results [4–6].

In this report, the processes within the converter are analyzed using an expanded harmonic analysis that includes a higher number of harmonics. The GNU Octave software version 9.2.0 environment is used for this purpose. Power calculations at the respective operating frequencies are performed using a relatively simple algorithm. This approach provides a deeper understanding of the actual load conditions experienced by the circuit components.

The main objective of the presented study is to provide a comparison between the first harmonic approximation (FHA), which is widely used for analysis, and higher-order

Check for updates

Academic Editors: Teodor Iliev, Ivaylo Stoyanov, Grigor Mihaylov and Selahattin Kosunalp

Published: 3 September 2026

Copyright: © 2026 by the authors. Licensee MDPI, Basel, Switzerland. This article is an open access article distributed under the terms and conditions of the Creative Commons Attribution (CC BY) license.

harmonic approximation. The authors sustain its application for power characteristics of resonant converters. The presented approach completes the area between calculation and circuit behavior investigation, which is crucial for optimal circuit design. The main goal of this study is to show that, through a relatively lightweight computational procedure, more accurate and practically relevant power estimations in the converter circuit can be obtained than those yielded by standard FHA-based analysis. Therefore, the presented method can be used for further data accuracy modeling and improved project design.

2. Power Analysis of the Series-Resonant Converter

2.1. Fourier Analysis of a Full-Bridge Series-Resonant Converter

A circuit of a full-bridge voltage-switching series-resonant converter is depicted in Figure 1. It consists of four controllable switches, a series-resonant circuit, and a high-frequency rectifier. The way of obtaining DC output from the circuit shown in Figure 1 is to insert a low-pass filter after the rectifier. It is assumed that the circuit response is instant and there are no switching losses. Fourier circuit analysis is used to determine the voltage and current values in different circuit branches. With its application, it is possible to obtain results about average power analysis. Energy and efficiency determination is presented separately to input source power, output (load) power, and resonant stage power.

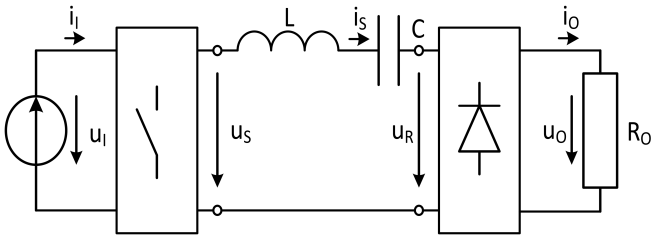


Figure 1. Series-resonant converter.

2.2. Power of the Resonant Circuit

The instantaneous value of the resonant branch voltage, which has a square waveform, could be determined as follows:

$$u_S(t) = \sum_{n=1}^{\infty} \frac{4U_I}{(2n-1)\pi} sin\Big[(2n-1)\omega_f t\Big], \quad (1)$$

where ω_f is the main frequency.

The instantaneous value of the resonant current is

$$i_S(t) = \sum_{n=1}^{\infty} I_{Sm(n)} sin\Big[(2n-1)\omega_f t + \psi_{I_S(n)}\Big], \quad (2)$$

where the components are as follows:

$\dot{I}_{Sm(n)} = \frac{\dot{U}_{Sm(n)}}{Z_{(n)}} = I_{Sm(n)} e^{j\psi_{I_S(n)}}$—complex amplitude of the current for the n-th harmonic number;

$Z_{(n)} = R + Z_{L(n)} + Z_{C(n)}$—equivalent impedance for the n-th harmonic number;

$\dot{U}_{Sm(n)} = \frac{4U_I}{(2n-1)\pi}$—complex amplitude of the voltage input for the n-th harmonic number, determined with Fourier analysis of the square wave [2].

Established values of each voltage and current harmonic numbers could define the complex power through

$$\dot{S}_{S(n)} = \dot{U}_{S(n)} \overline{I}_{S(n)} = P_{S(n)} + jQ_{S(n)} = S_{S(n)} e^{j\varphi_{(n)}}, \quad (3)$$

where the components are as follows:

$\dot{U}_{S(n)}$ is the complex value of the n-th voltage harmonic number;
$\bar{I}_{S(n)}$ is the conjunction value of the n-th current harmonic number;
$P_{S(n)}$ is the active power of the n-th harmonic number;
$Q_{S(n)}$ is the reactive power of the n-th harmonic number;
$S_{S(n)}$ is the apparent power of the n-th harmonic number;
$\phi_{(n)}$ is the phase angle between the current and voltage for the n-th harmonic number.
Total active, reactive and apparent power can be determined from

$$P = \sum_{n=1}^{\infty} P_{(n)};\ Q = \sum_{n=1}^{\infty} Q_{(n)};\ S = \sum_{n=1}^{\infty} S_{(n)}. \tag{4}$$

The resonant branch instantaneous power could have the following expression:

$$p_S(t) = u_S(t) i_S(t). \tag{5}$$

Figure 2 shows the relation of $u_{S(t)}$, $i_{S(t)}$ and $p_{S(t)}$ at Q_L = 2.5 and ν = 1.3 at relative units, where the base values are $U_b = U_{Sm(1)}$; $I_b = I_{Sm(1)}$; and $P_b = U_b I_b$. In the same figure, a comparison of instantaneous power $p_{S(1)}$ is given, determined by a first harmonic approximation. There is a significant deviation between both curves.

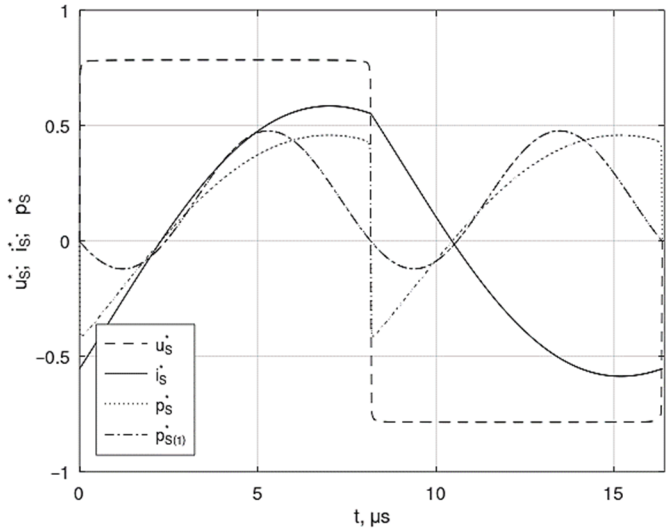


Figure 2. Resonant voltage, current and power waveforms for Q_L = 2.5 and ν = 1.3.

2.3. Input Power

With the usage of the harmonic analysis method, input values could have the following expression:

$$u_I(t) = U_I; \tag{6}$$

$$i_I(t) = I_I + \sum_{n=1}^{\infty} I_{Im(n)} sin\left[(2n-1)\omega_{fI} t + \psi_{I_I(n)}\right] \tag{7}$$

where U_I and I_I are the DC components of the voltage and current and $I_{Im(n)}$ and $\psi_{II(n)}$ are the amplitude and phase angle of the n-th harmonic, determined through Fourier series analysis. The cycle of the input current is twice the operating frequency [1]:

$$T_{fI} = T_f/2;\ \omega_{fI} = 2\omega_f \tag{8}$$

For input instantaneous power, we have

$$p_I(t) = u_I(t) i_I(t) = U_I i_I(t) \tag{9}$$

Figure 3 represents voltage, current and power on the input of the convertor at Q_L = 2.5 and ν = 1. There is also a comparison given of the total instantaneous power p_S, calculated by Fourier series and first harmonic approximation $p_{S(1)}$.

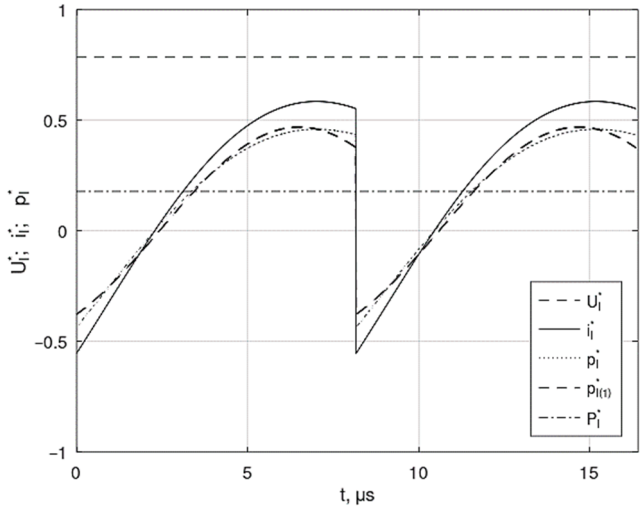


Figure 3. Input voltage, current and power waveforms for Q_L = 2.5 and ν = 1.3.

2.4. Output Power

Output current is determined by the resonant current when the switching sequence alters the polarity due to the switching periods. According to the Fourier analysis, the output current is

$$i_O(t) = I_O + \sum_{n=1}^{\infty} I_{Om(n)} sin\left[(2n-1)\omega_{fI}t + \psi_{I_O(n)}\right] \tag{10}$$

where I_O is the DC component of the current and $I_{Om(n)}$ and $\psi_{IO(n)}$ are the amplitude and phase angle of the n-th harmonic, determined through Fourier series analysis. To define the DC component of the active power, we use the following expression:

$$P_O = R_O I_O^2 \tag{11}$$

For the n-th harmonic of complex power, we determine:

$$\dot{S}_{O(n)} = \dot{U}_{O(n)}\overline{I}_{O(n)} = R_O\dot{I}_{O(n)}\overline{I}_{O(n)} = R_O I_{O(n)}^2 = P_{O(n)} \tag{12}$$

where $I_{O(n)}$ is the RMS value of the n-th harmonic. From the expression we could determine that the complex power of the n-th harmonic is equal to the active power. Total active power can be derived by

$$P_O = \sum_{n=0}^{\infty} P_{O(n)} \tag{13}$$

The instantaneous output power then is calculated by

$$p_O(t) = R_O i_O(t)^2 \tag{14}$$

where $i_O(t)$ is the instantaneous output current and R_O is output load active resistance.

Figure 4 represents the current and power on the output of the convertor at Q_L = 2.5 and ν = 1. There is also a comparison given of the total instantaneous power p_O, calculated by Fourier series and first harmonic approximation $p_{O(1)}$. The same plot also shows the DC component of the active power.

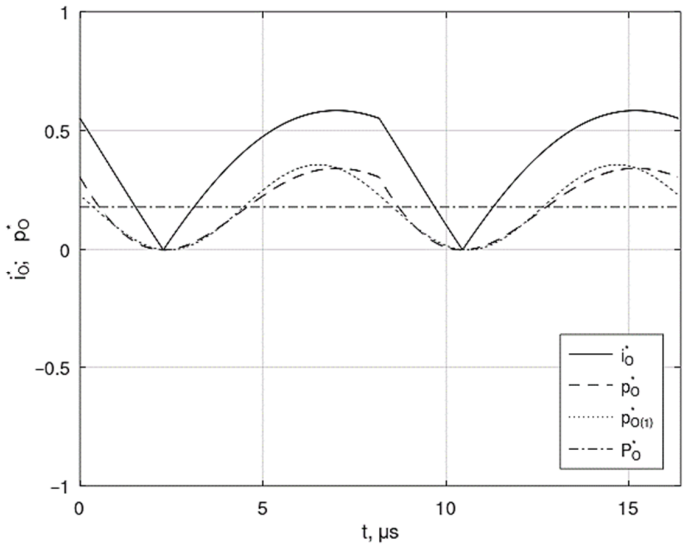


Figure 4. Output voltage, current and power waveforms for Q_L = 2.5 and ν = 1.3.

3. Experimental Results

The installation device was built with a control signal board, gate driver section and switching power stage. The applied control system is TMS320C2000 with F2808 DSP. It is a 32-bit fixed point processor with a clock set at 100 MHz, which provides frequency control with three modulation methods of the input signal.

The gate driver is unified model configuration, which delivers the necessary pulse sequence to the power switches while keeping the necessary electrical insulation by the usage of optocouplers. The output stage is implemented with MOSFET transistors in full-bridge layout. Its output is connected to a series-resonant LC circuit with rated values of L = 60 μH and C = 220 nF.

Resonant frequency of the experimental device is 44 kHz. The ail power supply is 32VDC. The characteristic load impedance is 16.4 Ω.

The measuring tool used is digital oscilloscope model Instek GDS-1102A-U with a range of 100 MHz and a sampling rate of 1 G Sa/s.

The laboratory prototype's block diagram and its main components are given in Figure 5. Here, its main application is for the tested series-resonant converter.

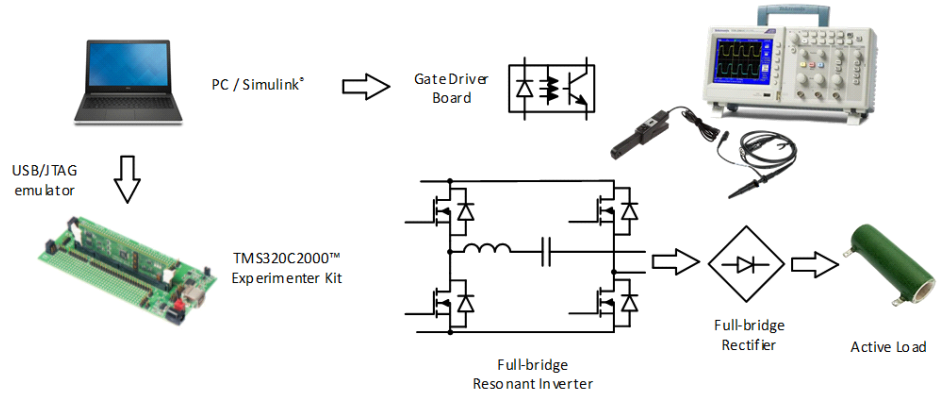


Figure 5. Block diagram of the experimental unit.

As it has already been described above, the main aim of the present study is to get data accuracy from the applied method. Therefore, power characteristics wee extracted from the laboratory prototype and are presented below.

Figures 6 and 7 show the waveforms, measured by a digital oscilloscope, of resonant voltage (yellow), current (blue) and power (red) plots at Q_L = 0.8, rated to a load impedance R_O = 18 Ω and Q_L = 2 and rated to a load impedance R_O = 5 Ω, and normalized frequencies of ν 1 and 1.3 accordingly. These values were measured at a rated frequency of 44.13 kHz и 57.38 kHz.

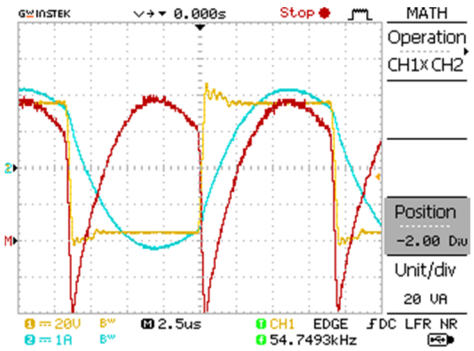


Figure 6. Resonant voltage, current and power waveforms for Q_L = 0.8 and ν = 1.3.

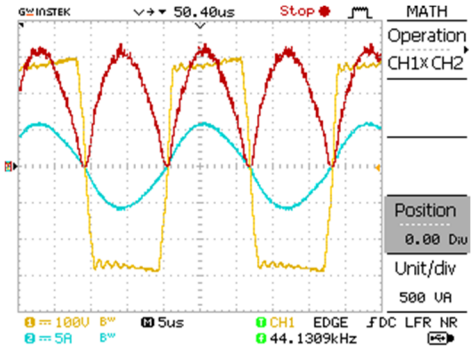


Figure 7. Resonant voltage, current and power waveforms for Q_L = 2.5 and ν = 1.

Figure 8 shows the waveforms, measured by digital oscilloscope, of the input voltage (yellow), current (blue) and power (red) plots at a quality factor Q_L = 2.5 and a normalized frequency ν = 1.

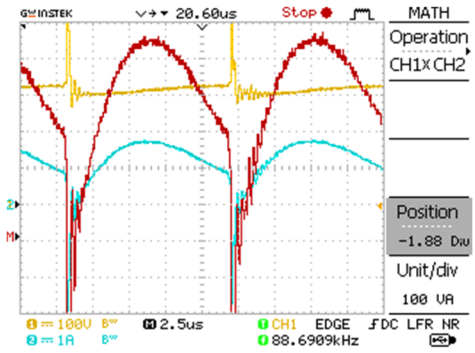


Figure 8. Input voltage, current and power waveforms for Q_L = 2.5 and ν = 1.

Figure 9 presents the waveforms, measured by digital oscilloscope, of the output voltage (yellow), current (blue) and power (red) plots at a quality factor Q_L = 0.8 and a normalized frequency ν = 1.

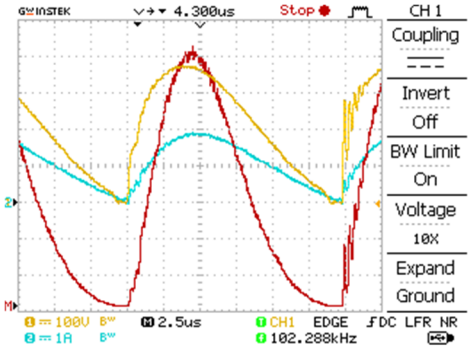


Figure 9. Output voltage, current and power waveforms for Q_L = 0.8 and ν = 1.

4. Conclusions

Derived mathematical data are then compared to those obtained from a real experimental model of a series-resonant converter. The presented experimental results in Figures 6–9 confirm the effectiveness of Fourier series analysis in resonant power converters, which delivers a higher accuracy than the classical first harmonic approximation (FHA). By including higher-order harmonics in the analysis, a more precise representation of circuit behavior was achieved, as is shown in Figures 2–4. The recorded discrepancies demonstrate the value of a more precise approach to power evaluation, which in turn leads to improved efficiency and reliability—not only of the converter itself but also of the overall system.

Possible study extensions could address circuit internal losses and switching non-idealities, which are crucial for renewable energy and battery power applications. Furthermore, extracted data could have an impact on proper circuit design and output filter estimation.

Author Contributions: Conceptualization, D.S., V.M., Y.M. and H.V.; methodology, D.S., V.M., Y.M. and H.V.; software, D.S., V.M., Y.M. and H.V.; validation, D.S. and H.V.; formal analysis, V.M., Y.M. and H.V.; investigation, Y.M. and H.V.; resources, D.S. and H.V.; data curation, D.S., V.M., Y.M. and H.V.; writing—original draft preparation, D.S., Y.M. and H.V.; writing—review and editing, D.S. All authors have read and agreed to the published version of the manuscript.

Funding: This research received no external funding.

Institutional Review Board Statement: Not applicable.

Informed Consent Statement: Not applicable.

Data Availability Statement: The original contributions presented in this study are included in the article. Further inquiries can be directed to the corresponding author.

Acknowledgments: The work presented in this paper has been supported by "Science" Fund at University of Food Technologies—Plovdiv, Bulgaria.

Conflicts of Interest: The authors declare no conflicts of interest.

References

1. Kazimierczuk, M.K.; Czarkowski, D. *Resonant Power Converters*, 2nd ed.; Wiley: Hoboken, NJ, USA, 2011.
2. Hart, D. *Power Electronics*; McGraw-Hill: New York, NY, USA, 2011.
3. Hinov, N.; Hranov, T. Development of series resonant converter models with output transformer. In *Proceeding of the 2017 XXVI International Scientific Conference Electronics (ET), Sozopol, Bulgaria, 13–15 September 2017*; IEEE: Piscataway, NJ, USA, 2017; pp. 1–4. [CrossRef]
4. Mukherjee, S.; Barbosa, P. Design and Optimization of an Integrated Resonant Inductor with High-Frequency Transformer for Wide Gain Range DC–DC Resonant Converters in Electric Vehicle Charging Applications. *IEEE Trans. Power Electron.* **2023**, *38*, 6380–6394. [CrossRef]

5. Cho, Y.-J.; Kim, N.-Y.; Lee, K.-J. A Simplified Equivalent Circuit Model of a Phase-Shift Series Resonant Converter. *Electronics* **2026**, *15*, 1491. [CrossRef]
6. M'barki, Z.; Senhaji Rhazi, K.; Mejdoub, Y. A novel fuzzy logic control for a zero current switching-based buck converter to mitigate conducted electromagnetic interference. *IJECE* **2023**, *13*, 1423–1436. [CrossRef]

Disclaimer/Publisher's Note: The statements, opinions and data contained in all publications are solely those of the individual author(s) and contributor(s) and not of MDPI and/or the editor(s). MDPI and/or the editor(s) disclaim responsibility for any injury to people or property resulting from any ideas, methods, instructions or products referred to in the content.

https://doi.org/10.3390/engproc2026154080